

The Covariance Matrix for Radar Imaging of Targets Buried Beneath Two-Dimensional Rough Surfaces

¹Magda El-Shenawee and ²Eric Miller

¹University of Arkansas

Department of Electrical Engineering

Fayetteville, AR 72701

magda@uark.edu

²Northeastern University

Department of Electrical and Computer Engineering

Boston, MA 02115

emiller@neu.edu

ABSTRACT

In this work, radar images of dielectric targets buried beneath 2-D rough ground surfaces are simulated. These images are based on the amplitude and phase of all polarizations of incident and scattered waves. Both bistatic and backscatter intensity-based images are considered in this work to compare the image quality in each case. All simulations are obtained using the integral equation based technique; the Steepest Descent Fast Multipole method (SDFMM). The numerical results show that images based on the Covariance matrix are very unique when the surrounding illuminated areas have almost the same rough surface profile. However, these images deteriorate as the surface profile greatly changes in the surrounding ground areas.

Keywords: Radar Polarimetry, detection of buried objects, backscatter intensity, imaging of buried penetrable targets, rough surface scattering.

1. INTRODUCTION

In previous work [1]-[3], a variety of 3-D scattering problems were investigated. These papers focused on analyzing the electromagnetic wave scattering from dielectric and/or perfect electric conductor (PEC) objects buried beneath 2-D random rough surfaces. The results of these papers helped in understanding the physics involved in the buried object application. However, the ultimate goal is to detect the buried targets. It is clear from [1]-[3] that the ground roughness greatly obscures the target's signature which is often much smaller than the ground signature. The current work attempts to develop a detection technique based on the physics of the electromagnetic wave scattering mechanism. In particular, the proposed technique is based on the depolarization of the electromagnetic waves scattered from a target buried beneath the rough surface ground. The fully polarimetric scattering matrix S is given by [4]:

$$\begin{bmatrix} E_v^s \\ E_h^s \end{bmatrix} = \frac{e^{jkr}}{r} \begin{bmatrix} S_{vv} & S_{vh} \\ S_{hv} & S_{hh} \end{bmatrix} \begin{bmatrix} E_v^i \\ E_h^i \end{bmatrix} \quad (1)$$

where i and s represent the incident and scattered waves, respectively. The symbols v and h represent the vertically and horizontally polarized waves, respectively. The Covariance matrix C is given by [4]:

$$\overline{C} = \begin{bmatrix} S_{vv}S_{vv}^* & S_{vv}S_{vh}^* & S_{vv}S_{hv}^* & S_{vv}S_{hh}^* \\ S_{vh}S_{vv}^* & S_{vh}S_{vh}^* & S_{vh}S_{hv}^* & S_{vh}S_{hh}^* \\ S_{hv}S_{vv}^* & S_{hv}S_{vh}^* & S_{hv}S_{hv}^* & S_{hv}S_{hh}^* \\ S_{hh}S_{vv}^* & S_{hh}S_{vh}^* & S_{hh}S_{hv}^* & S_{hh}S_{hh}^* \end{bmatrix} \quad (2)$$

In general, the covariance matrix is complex with sixteen elements, but in the backscatter direction they are reduced to nine complex elements. However, the computational effort is not consumed in the covariance matrix calculations but is consumed in computing the radar cross section at each pixel in the image. In this work, we use the well developed solver based on the steepest descent fast multipole method (SDFMM) to compute the surface currents on the ground and buried target and hence to compute the radar cross section of the whole scatterer. This model has been successfully used to analyze the 3-D scattering problems, in particular, the 2-D random rough ground surfaces with multiple buried targets [1]-[3]. The SDFMM computer code is used to calculate the fully polarimetric matrix elements, i.e. the vv , hh , vh and hv scattered fields, given in eq. (1) for hundreds of randomly generated rough surface realizations with and without the buried target. Then, the covariance matrix is computed at each pixel of the image. The images are displayed for both the backscatter and bistatic directions. Producing images based on all the sixteen elements of the Covariance matrix provides the most enhanced image of the target. The configuration of the problem is given in Fig. 1.

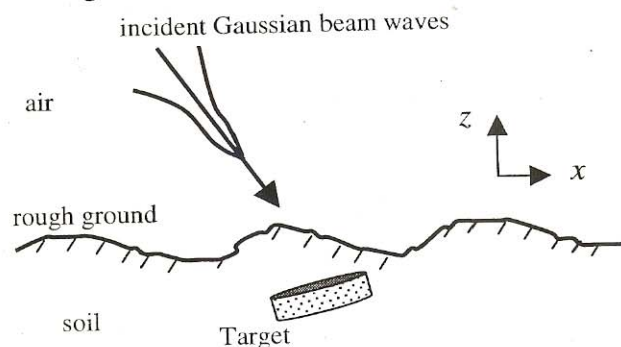


Figure 1. Cross section of 2-D rough ground with buried Target (3-D scattering).

2. NUMERICAL RESULTS

This Section presents several radar images of targets buried beneath the rough ground. These images are composed of number of pixels, at which the amplitude is equal to the radar cross section.

The radar illuminates several spots on the ground (i.e. scanning) as shown in Fig. 2. Each ground area scatters power which represents the amplitude at one pixel.

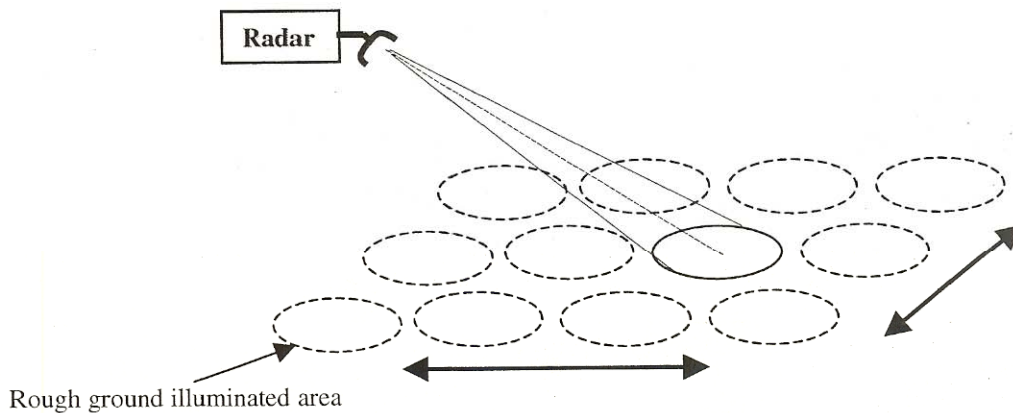


Figure 2. Radar Beam Illumination.

The rough surface is characterized by Gaussian statistics. The rms height and the correlation length of the rough ground are assumed as $\sigma = 0.1\lambda_0$ and $l_c = 0.5\lambda_0$, respectively. The dimensions of the ground are $8\lambda_0 \times 8\lambda_0$ with Gaussian half-beam width equal to $1.6\lambda_0$ centered on the ground at $4\lambda_0 \times 4\lambda_0$, where λ_0 is the free space wavelength [1]. The buried object is assumed a disk with radius and height as $a = 0.3\lambda_0$, and $h = 0.1\lambda_0$, respectively. Four orientations for the object are considered here with Euler's angles as $(0, 20, 0)$, $(10, 10, 0)$, $(10, 0, 10)$ and $(0, 0, 0)$, respectively. The relative dielectric constants of the ground and disk are assumed $\epsilon_r = 2.5 - j0.18$, $\epsilon_r = 4.0$, respectively. The disk is buried at $z = -0.3\lambda_0$ measured from the center of its top circular surface.

Numerical results for images based on the sixteen complex Covariance matrix elements are computed and presented in Figs. 3-8 (all results are on log-scale). The formulations can be found in previous work [1]-[3]. The results in Figs. 3-4 are for normal incidence, while they are for oblique incidence at $\vartheta^i = 10^\circ$ and $\varphi^i = 0^\circ$ in Figs. 5-7. In all figures, the real and/or the imaginary parts of four elements of C are presented for 4 targets buried under the random rough ground. In Figs. 3-6, it is assumed that the surrounding illuminated rough ground areas have the same rough surface profile (see Fig. 2). The results in Fig. 3 clearly show the four targets only when the elements C_{34} , C_{24} and C_{31} are investigated. Other elements of C were also useful (not presented here). However, images based on C_{11} (i.e. co-polarized waves) did not help in detecting the targets as shown in Fig 3. It is important to emphasize that no subtraction of the background was processed in these results. Figure 4 shows the same images of Fig. 3 but when the four objects were buried beneath a sinusoidal ground. In this case, the period and height of the ground are $1\lambda_0$ and $0.2\lambda_0$, respectively. Figure 5 shows the same images of Fig. 3 but at oblique incidence ($\vartheta^i = 10^\circ$ and $\varphi^i = 0^\circ$). In all above results, no noise was added to the simulations. On the other hand, in Fig. 6, images based on the imaginary part of C_{12} are presented upon adding random noise. Fig. 6a has

zero noise while Figs. 6b-d have random noise ranges from 1-1.4%. In Fig. 7, additive noise represented by inserting different rough surface profiles in the illuminated ground areas. The roughness parameters of these profiles are $\sigma = 0.09\lambda_0$ and $\sigma = 0.08\lambda_0$ with the same correlation length as before. Fig. 7 clearly shows the need to develop a technique for removing these additive noise.

The presented results clearly show that images based on the Covariance elements C_{34} , C_{24} , C_{31} , C_{12} , C_{31} etc., can significantly help in detecting the buried targets. However, the images based on C_{11} and C_{44} (i.e. the co-polarized waves) almost do not show the buried targets as demonstrated in Figs. 3-6. In addition, when the surrounding rough ground areas have different rough surface profiles, the images become very obscured (noisy) and do not show the buried objects.

3. CONCLUSIONS

This work presents radar images of penetrable targets buried beneath the rough surface ground. The results show that examining all the Covariance matrix elements greatly help in producing clear images of the buried targets. However, if the radar images are based only on the co-polarized scattered waves, the images become unclear. This work can help in enhancing the radar-based detection techniques.

ACKNOWLEDGMENTS

This research was sponsored in part by the Northeastern University NSF-ERC award number EEC-9986821 and in part by the Arkansas Science and Technology Authority Grant No AR/ASTA/01-B-18.

REFERENCES

1. M. El-Shenawee, C. Rappaport, E. Miller and M. Silcivitch, "Three-dimensional subsurface analysis of electromagnetic scattering from penetrable/PEC objects buried under rough surfaces: use of the steepest descent fast multipole method (SDFMM)," *IEEE Trans. Geosci. & Rem. Sensing*, vol. 39, no. 6, pp. 1174-1182, June 2001.
2. M. El-Shenawee and C. Rappaport, "Monte Carlo Simulations for the Statistics of Clutter in Minefields: AP Mine-Like Target Buried Near a Dielectric Object Beneath Two-Dimensional Randomly Rough Ground," *IEEE Trans. Geosci. & Rem. Sensing*, vol. 40, no. 6, pp. 1416-1426, June 2002.
3. M. El-Shenawee, "Scattering from Multiple Objects Buried Under Two-Dimensional Randomly Rough Surface using the Steepest Descent Fast Multipole Method," *IEEE Trans. Antennas and Propagations*, accepted for publication, to appear in March 2003.
4. F. T. Ulaby and C. Elachi, *Radar Polarimetry for Geoscience Applications*, Artech House, Inc., 1990.

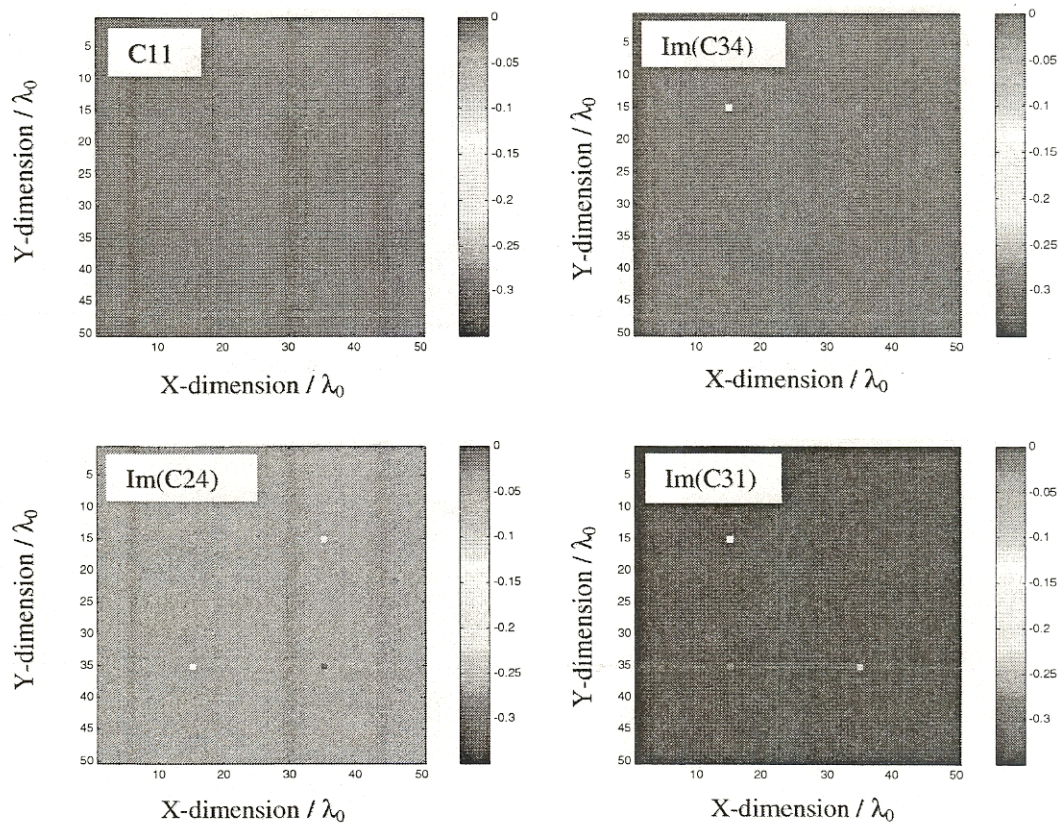


Figure 3. Images of 4 buried targets beneath random rough ground based on the Covariance matrix elements C_{11} , C_{34} , C_{24} and C_{31} . The roughness parameters are $\sigma = 0.1\lambda_0$ (rms height) and $l_c = 0.5\lambda_0$ (correlation length). Normal incidence at backscatter.

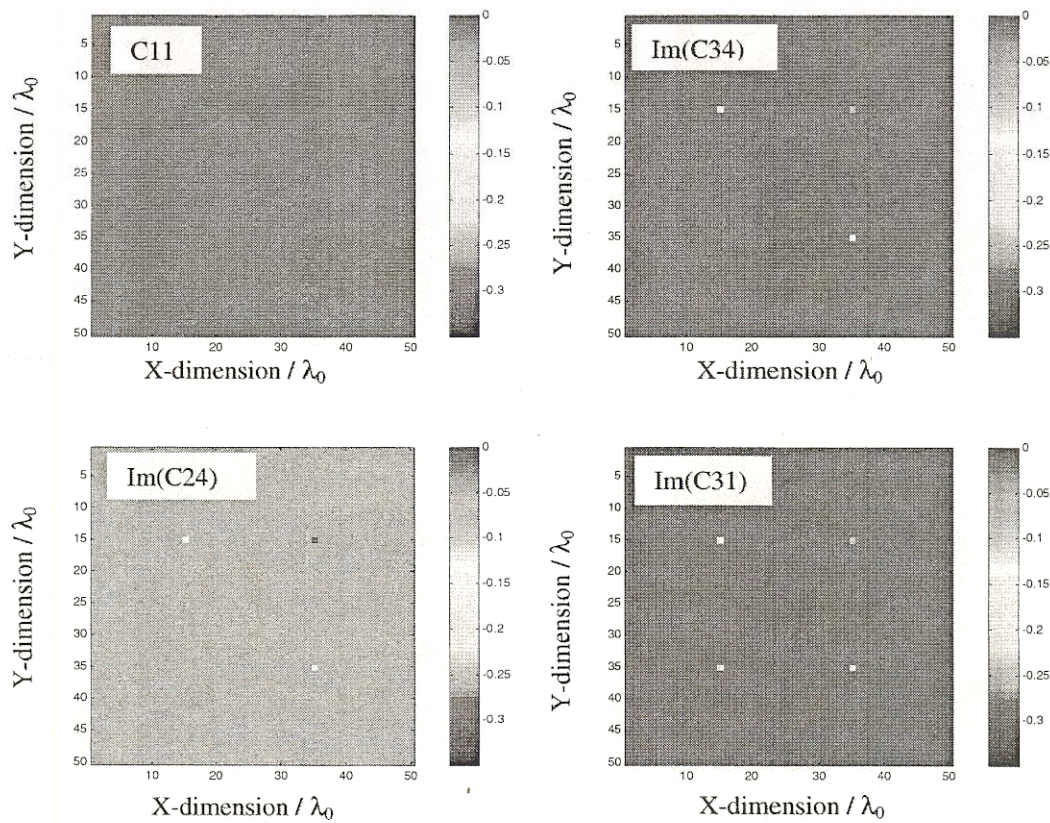


Figure 4. Images of 4 buried targets beneath sinusoidal rough ground based on the Covariance matrix elements C_{11} , C_{34} , C_{24} and C_{31} . The period and height of the rough surface are $1\lambda_0$ and $0.2\lambda_0$, respectively. Normal incidence at backscatter.

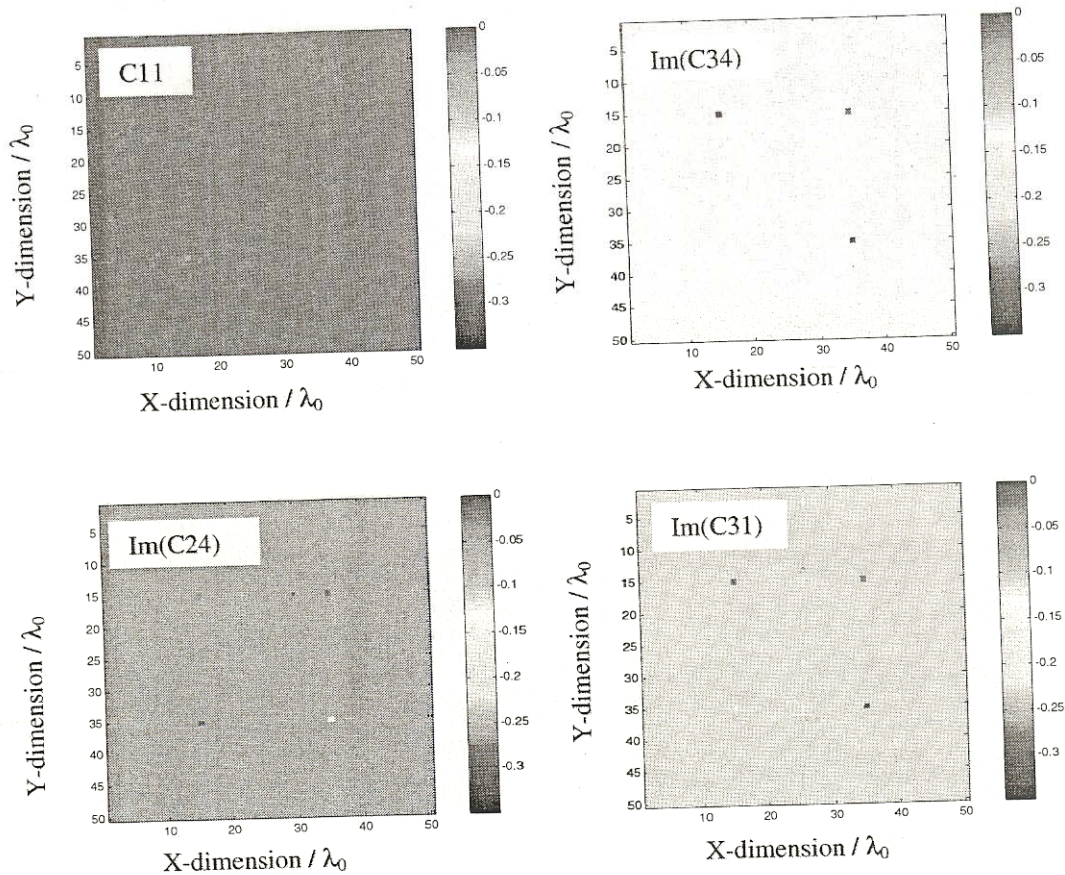


Figure 5. Images of 4 buried targets beneath random rough ground based on the Covariance matrix elements C_{11} , C_{34} , C_{24} and C_{31} at backscatter direction. The roughness parameters are $\sigma = 0.1\lambda_0$ (rms height) and $l_c = 0.5\lambda_0$ (correlation length). Oblique incidence at $\vartheta^i = 10^\circ$ and $\varphi^i = 0^\circ$.

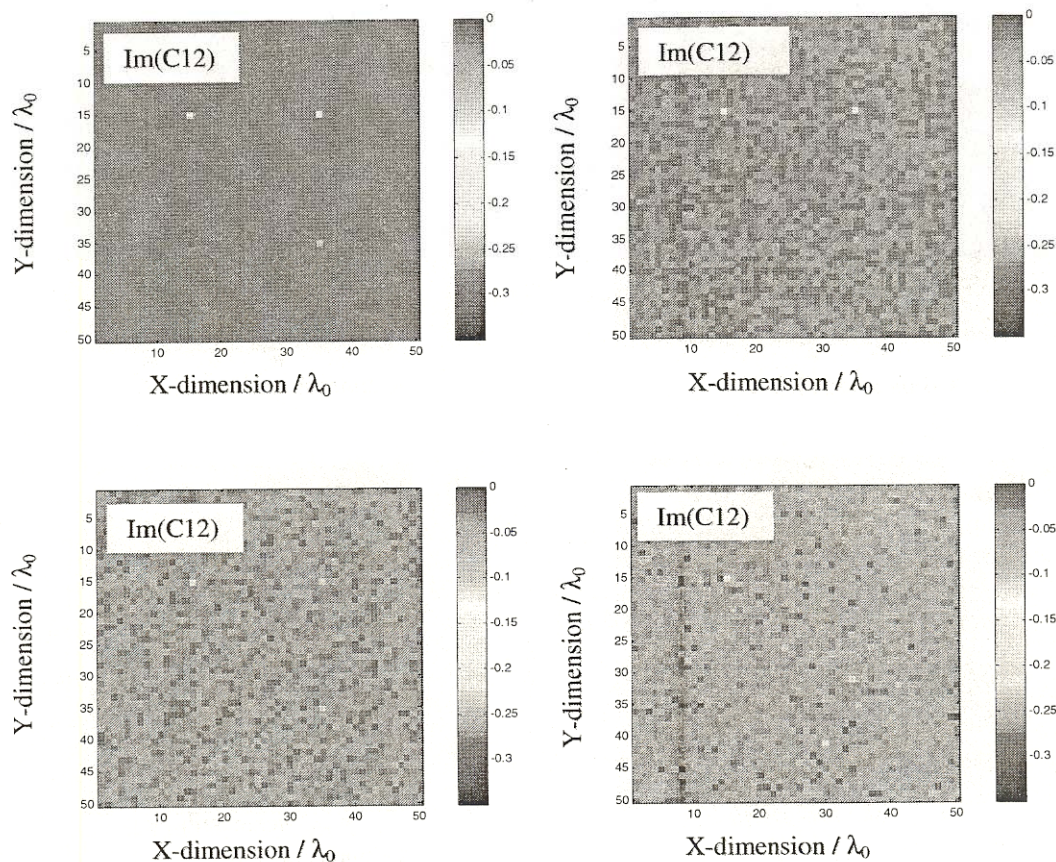


Figure 6. Images of 4 buried targets beneath random rough ground based on the Covariance matrix elements C_{12} at backscatter direction upon adding random noise at (a) 0, (b) 1%, (c) 1.15% and (d) 1.41%. The roughness parameters are $\sigma = 0.1\lambda_0$ (rms height) and $l_c = 0.5\lambda_0$ (correlation length). Oblique incidence at $\vartheta^i = 10^\circ$ and $\varphi^i = 0^\circ$.

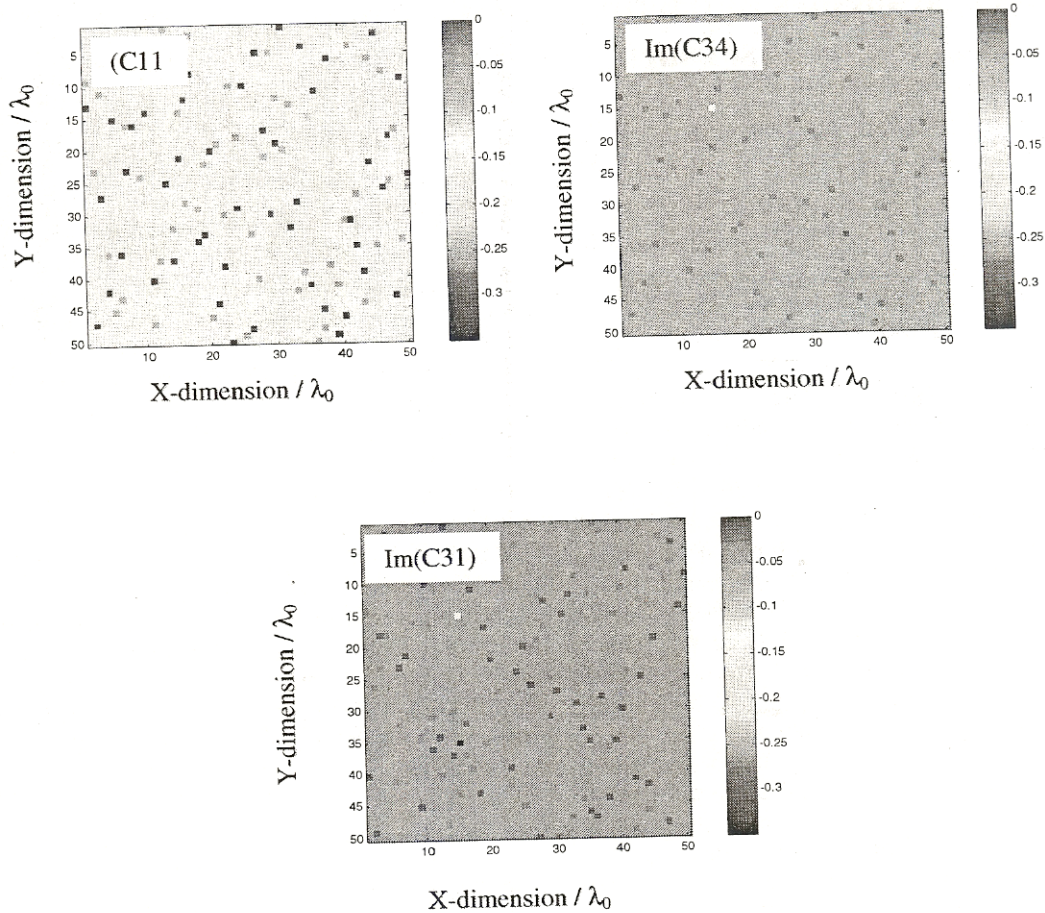


Figure 7. Images of 4 buried targets beneath random rough ground based on the Covariance matrix elements C_{11} , C_{34} and C_{31} at backscatter direction. Adding additive noise. The roughness parameters are $\sigma_1 = 0.1\lambda_0$, $\sigma_2 = 0.09\lambda_0$, $\sigma_3 = 0.08\lambda_0$ and $l_{c1,2,3} = 0.5\lambda_0$. Oblique incidence at $\vartheta^i = 10^\circ$ and $\varphi^i = 0^\circ$.